ELSEVIER

Journal of Nuclear Materials 313–316 (2003) 657–663

journal of nuclear materials

www.elsevier.com/locate/jnucmat

Scaling of ITER divertor parameters – interpolation from 2D modelling and extrapolation

H.D. Pacher [a,*], A.S. Kukushkin [b], G.W. Pacher [c], G. Janeschitz [d]

[a] *INRS-Energie, Matériaux, et Télécommunciations, 1650 Boul. Lionel Boulet CP 1020, Varennes, Que., Canada*
[b] *ITER Joint Central Team, Garching Joint Work Site, Garching, Germany*
[c] *Hydro_Québec, Varennes, Que., Canada*
[d] *Forschungszentrum Karlsruhe, Karlsruhe, Germany*

Abstract

Detailed modelling studies of the divertor plasma for ITER have been carried out. Using these results, scaling relationships are developed linking SOL power, density, throughput, pumping speed, peak divertor power load, and helium density for ITER conditions in order to systematise the results and to extrapolate them beyond the range presently covered by the simulations. The key parameter for the scalings is the neutral pressure in the divertor. Both peak power load and helium density vary as the square of the power at constant pressure. The inclusion of helium elastic collisions reduces the helium density and leads to a steeper reduction with increasing pressure. Variants of the input conditions, i.e. different geometry, no helium elastic collisions, carbon walls, are also discussed, the consistency of the edge modelling with conditions required in the core is treated, and extrapolation to higher power operation is carried out.

Keywords: ITER; Divertor; Plasma; Tokamak; B2-EIRENE; ASTRA

1. Introduction

B2–EIRENE design studies of the ITER divertor have been carried out. The following set of conditions apply, except where variants (different geometry, no helium elastic collisions, carbon walls) are specified. The geometry is that of Fig. 1, with the divertor plates forming a V-shape near the strike points, realistic gas conductance between the inner and outer divertors [1,2], and a design pumping speed up to 75 m^3/s from the PFR (private flux region). The targets are carbon, the impurities are carbon and helium with all charge states at the same temperature. Carbon is released from the plates by both physical and chemical sputtering with 1% yield, and fully absorbed at the walls. Along the CEI (core–edge interface), electron and ion energy fluxes are uniform and equal, the helium flux equals the production rate, and other impurity fluxes are zero. Sheath boundary conditions apply at the plates, and the radial gradient length near the wall is set to 3 cm. Along-field transport is flux-limited and cross-field transport is determined by $D_\perp = 0.3$ m^2/s and $\chi_{e\perp} = \chi_{i\perp} = 1$ m^2/s, (for a more complete discussion see [2]). The plasma is fuelled by a combination of gas puff and net core flux (ions out-neutrals in). Elastic collisions of helium with DT atoms are included. The fusion power and SOL power are related by taking $Q = 10$ and a core radiation fraction f_{rad} of 30%; for other values of Q and f_{rad}, the helium production rate should be corrected by a factor $f_{He} = 0.21(5Q/(Q+5))(1-f_{rad})^{-1}$. The scaling relations in the present paper apply to partially attached plasmas in ITER with a V-shaped vertical target and carbon plates. (They supersede previous estimates [3], which used a simplified neutral model and applied to

* Corresponding author.
E-mail address: pacher@inrsener.uquebec.ca (H.D. Pacher).

0022-3115/03/$ - see front matter
PII: S0022-3115(02)01374-0

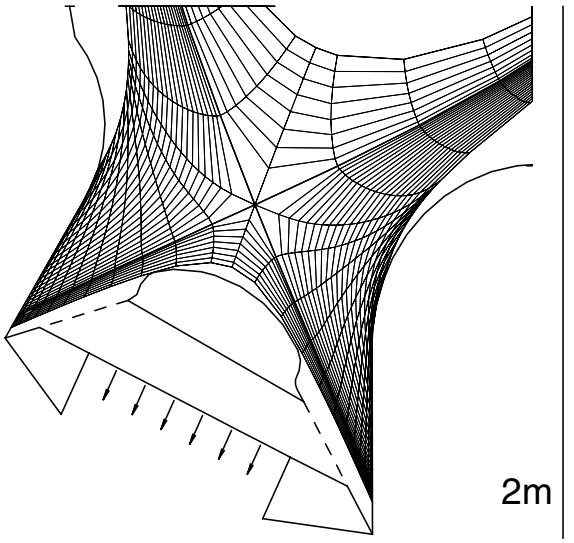

Fig. 1. Reference geometry of the ITER divertor having V-shaped divertor floor near strike point.

high recycling with reversed targets and without impurity radiation.)

2. Scaling relations

The relation between separatrix density and throughput for various powers, pumping speeds, and fuelling conditions is shown in Fig. 2. Each series exhibits a saturation in density as the throughput increases (see [1,2]), which is related to the progress of the inner divertor toward full detachment. This saturation may be due to the increase of volume recombination (see [4] for a theoretical analysis of a single divertor).

All these cases can be unified (Fig. 3) by expressing the normalised density as a function of the normalised average divertor neutral pressure (throughput over pumping speed) according to the scaling:

$$n_{\#}/(f_{\mathrm{fuel}}P_{\#}^{0.55}) = (\Gamma_{\#}/(S_{\#}P_{\#}^{0.87}))^{\alpha 1},$$
$$\alpha 1 = 0.36(\mathrm{A}) \text{ or } 0.02(\mathrm{B}), \quad (1)$$

where regime A, the 'normal' regime, occurs for $\Gamma_{\#} < S_{\#}P_{\#}^{0.87}$ and regime B, the saturated regime, for $\Gamma_{\#} > S_{\#}P_{\#}^{0.87}$. Very low and very high throughputs deviate from this scaling, but they are less interesting since they correspond to high peak power loads and full detachment, respectively. The separatrix midplane density n, throughput Γ, pumping speed S, SOL power P, peak power load q_{pk}, separatrix helium density $n_{\mathrm{He\_s}}$ and concentration $c_{\mathrm{He\_s}}$, and separatrix average density $n_{\mathrm{sep\_avg}}$, separatrix helium average density $n_{\mathrm{He\_sep\_avg}}$, electron temperature $T_{\mathrm{e\_sep\_avg}}$, ion temperature $T_{\mathrm{i\_sep\_avg}}$, and neutral flux $\Gamma_{\mathrm{DT0-sep}}$, are normalised respectively by: $n_0 = 0.333 \times 10^{20}$ m^{-3}, $\Gamma_0 = 124$ Pa m^3/s, $S_0 = 20$ m^{3}s^{-1}, $P_0 = 100$ MW, $q_{\mathrm{pk\_0}} = 7.55$ MW m^{-2}, $n_{\mathrm{He\_0}} = 0.00296 \times 10^{20}$ m^{-3}, $c_{\mathrm{He\_0}} = 0.00862$, $n_{\mathrm{sep\_avg\_0}} = 0.381 \times 10^{20}$ m^{-3}, $n_{\mathrm{He\_sep\_avg\_0}} = 0.0033 \times 10^{20}$ m^{-3}, $T_{\mathrm{e\_sep\_avg\_0}} = 165$ eV, $T_{\mathrm{i\_sep\_avg\_0}} = 280$ eV, and $\Gamma_{\mathrm{DT0-sep0}} = 16.4$ Pa m^3/s. The normalised quantities are denoted by a subscript # and are 1 at the transition between the two regimes when $P = P_0$ and $S = S_0$.

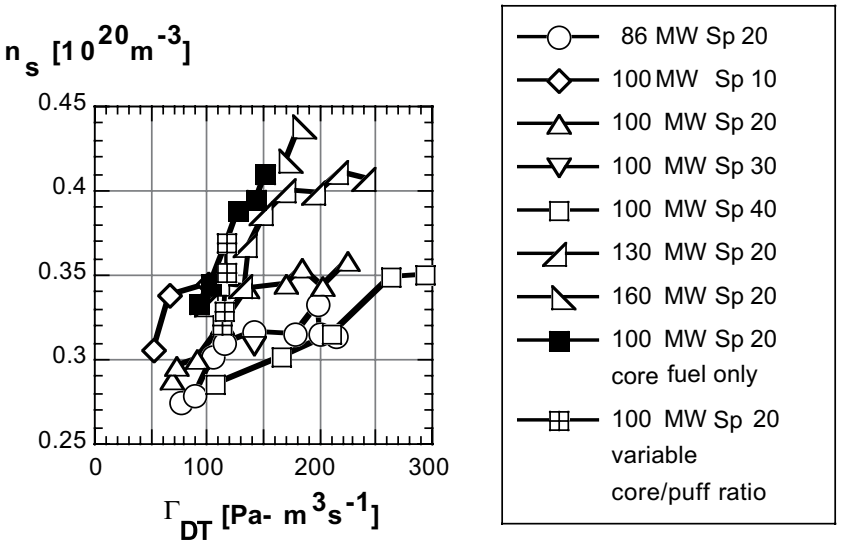

Fig. 2. Density at the separatrix midplane versus DT throughput, for SOL powers from 86 to 160 MW and pumping speeds Sp from 10 to 40 m^3/s. Fuelling mainly by gas puff (50–300 Pa m^3/s) with minor core fuelling (17 Pa m^3/s) except for (i) solid squares: core fuelling only and (ii) crossed squares: throughput 120 Pa m^3/s, variable gas puff.

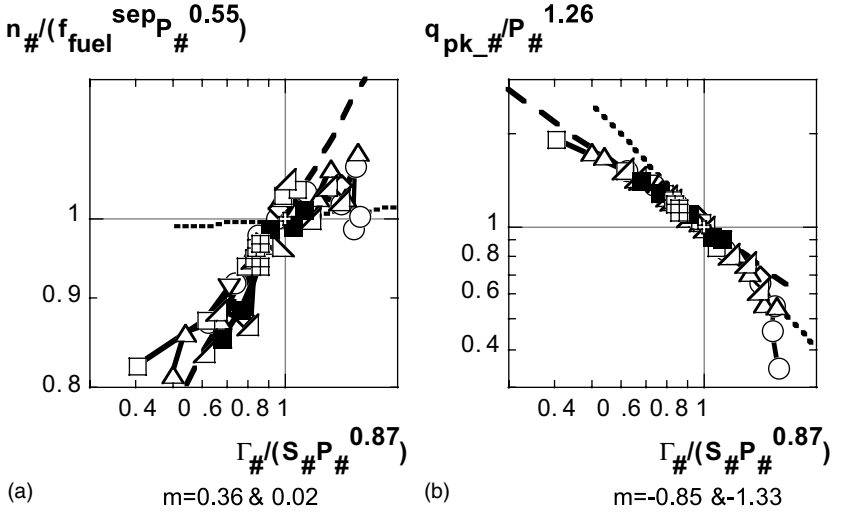

Fig. 3. (a) Normalised density and (b) normalised peak power load, versus normalised throughput (divertor pressure). Legend as in Fig. 2, dashed line scaling regime A, dotted scaling regime B, hollow cross transition point, slopes below figures.

To fit the core fuelled cases also, the factor $f_{\rm fuel} \equiv (\Gamma_{\rm puff} + 1.18(\Gamma_{\rm DT} - \Gamma_{\rm puff}))/\Gamma_{\rm DT}$ is introduced, i.e. the SOL is fuelled 18% more efficiently via the core than by the gas puff, plausible since core fuelling occurs via warm ions.

The peak power load (Fig. 3(b)) in the two regimes scales as

$$q_{\rm pk\_\#}/P_\#^{1.26} = (\Gamma_\#/(S_\# P_\#^{0.87}))^{\alpha 2},$$
$$\alpha 2 = -0.85(A) \quad \text{or} -1.33(B) \tag{2}$$

and the helium density (Fig. 4(a)) as:

$$\frac{n_{\rm He\_s} S_\# f_{\rm fuel}}{n_{\rm He\_0} P_\#^{0.26} f_{\rm He}} = (\Gamma_\#/(S_\# P_\#^{0.87}))^{\alpha 3},$$
$$\alpha 3 = -2(A) \quad \text{or} -1.75(B). \tag{3}$$

Scalings were also established for $n_{\rm sep\_avg}$, $T_{\rm e\_sep\_avg}$, $T_{\rm i\_sep\_avg}$, and $\Gamma_{\rm DT0-sep}$, but are not given here for space reasons.

All the values at the critical transition point increase with power:

$$n_{\#\_\rm crit} = f_{\rm fuel} P_\#^{0.55}, \quad \Gamma_{\#\_\rm crit} = P_\#^{0.87} \cdot S_\#,$$
$$q_{\rm pk\_\#\_crit} = P_\#^{1.26}, \quad n_{\rm He\_s\_crit}/n_{\rm He\_0} = f_{\rm He} P_\#^{0.26}/(f_{\rm fuel} S_\#) \tag{4}$$

but this is more critical for the peak power load, 7.75 MW/m^2 for 100 MW and increasing more strongly, than for the helium concentration, below 1% at 100 MW.

Collecting the dependences in the attached regime A, we have:

$$n_\# = P_\#^{0.24} f_{\rm fuel} (\Gamma_\# S_\#^{-1})^{0.36}, \quad n_{\rm sep\_avg\_\#} = 1.144 \cdot n_\#, \tag{5}$$

$$q_{\rm pk\_\#} = P_\#^2 (\Gamma_\# S_\#^{-1})^{-0.85},$$
$$n_{\rm He\_s}/n_{\rm He\_0} = P_\#^2 f_{\rm He} f_{\rm fuel}^{-1} S_\#^{-1} (\Gamma_\# S_\#^{-1})^{-2}. \tag{6}$$

Since integrated power and helium production vary as the fusion power, the peak power load and the helium density should increase at least linearly with power. Their variation with the square indicates steepening of the power profile and reduction of helium pumping with increasing power (e.g. because the plasma is hotter). They improve strongly with divertor pressure $\Gamma_\# S_\#^{-1}$, but this improvement is limited by the transition. Increased pumping speed benefits the helium density at constant pressure, and does not change the density or peak power load.

3. Helium elastic collisions

In the absence of helium elastic collisions with DT, the density and peak power load scalings are unchanged, but the helium density (Fig. 4(b)) scales as

$$\frac{n_{\rm He\_s}^{\rm noel} S_\# f_{\rm fuel}}{n_{\rm He0}^{\rm noel} P_\#^{1.13} f_{\rm He}} = (\Gamma_\#/(S_\# P_\#^{0.87}))^{\alpha 4},$$
$$\alpha 4 = -1(A) \quad \text{or} -0.85(B) \tag{7}$$

with $n_{\rm He0}^{\rm noel} = 0.0122 \times 10^{20}$ m^{-3}, and $c_{\rm He\_noel\_0} = 0.0366$. The scaling in regime A is

$$n_{\rm He\_noel\_s}/n_{\rm He\_noel\_0} = P_\#^2 f_{\rm He} f_{\rm fuel}^{-1} S_\#^{-1} (\Gamma_\# S_\#^{-1})^{-1} \tag{8}$$

i.e. the power dependence is the same as with the collisions, the helium density would be higher, and the helium density would decrease with increasing divertor

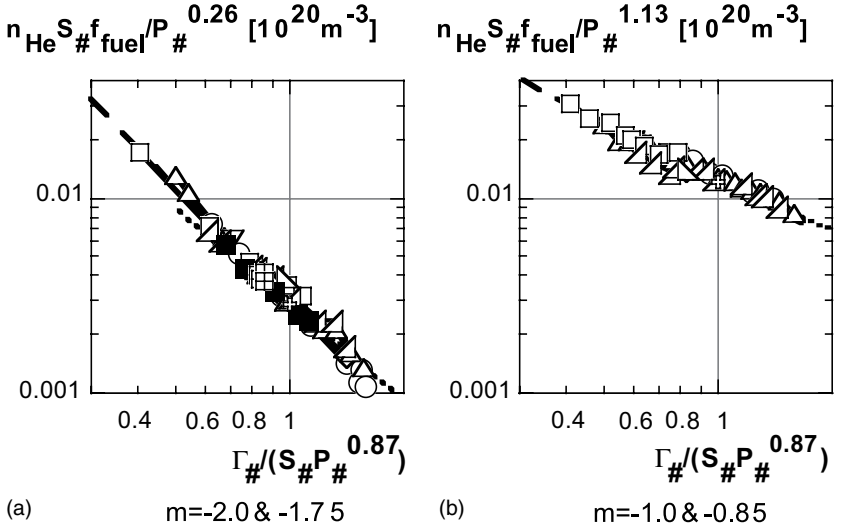

Fig. 4. Helium density (a) with helium elastic collisions on DT and (b) without these collisions, versus normalised throughput (divertor pressure). Legend Fig. 3.

pressure only as the first rather than as the second power. Inclusion of helium elastic collisions therefore has a profound effect.

4. Carbon walls

In contrast to walls which absorb completely (net deposition everywhere other than the target), as in the calculations above, full carbon walls represent the other, pessimistic, extreme. This leads to $Z_{\text{eff}} = 1.8$ (the standard cases are below 1.4), a density 14% below the scaling, a peak power load 37% below the scaling (Fig. 5), and unchanged helium density. Much more power is radiated in the SOL, 55% rather than 40%, leaving less power available for ionisation and consequently deposition on the plates.

5. Core-edge consistency

Core conditions are determined from the Integrated Core Pedestal Sol (ICPS) Model [5,6], using the separatrix temperatures and DT neutral fluxes for each

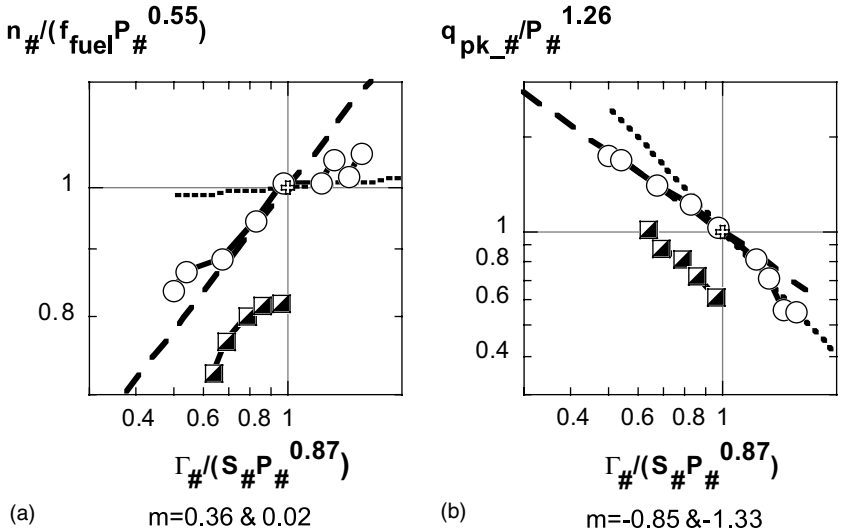

Fig. 5. (a) Normalised density and (b) normalised peak power load, versus normalised throughput (divertor pressure) for 100 MW and $S_p = 20$ m^3/s with absorbing walls (hollow circles) and carbon walls (half-filled squares).

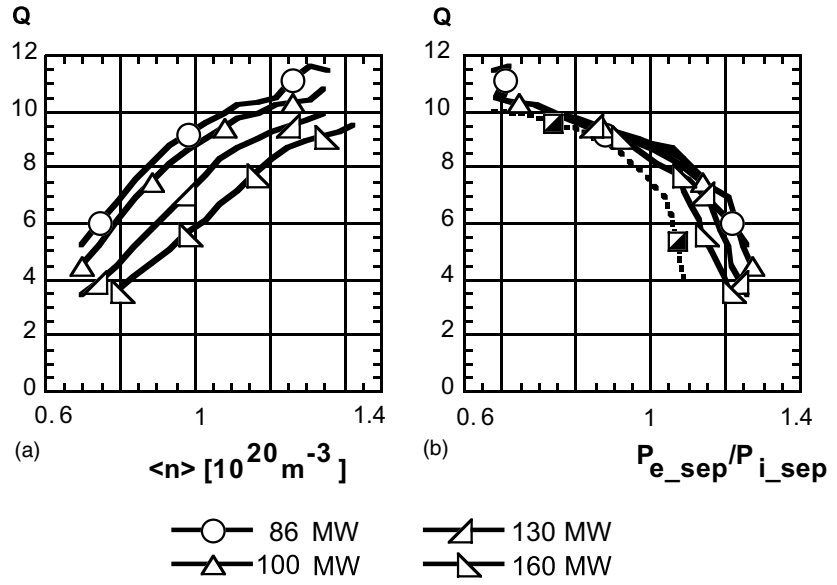

Fig. 6. Fully-relaxed core operation from ICPS model with boundary conditions from 2-D modelling. (a) Q versus average core density for varying SOL power at $n_s = 0.82 n_{crit}$. (b) Q versus ratio of power conducted by electrons to that by ions for same conditions; dashed line is $P_{SOL} = 100$ MW, $n_s = 0.94 n_{crit}$.

power and separatrix density given by the 2D scalings as boundary conditions (the helium parameters were not yet scaled). The SOL power is set to the desired value by controlling the auxiliary power. At each P_{SOL}, n_s is set to a fixed ratio n_s/n_{s_crit} (Eq. (4)) of 0.82 or 0.94 (Fig. 6), and the core density is then varied by varying the core fuelling. For equal ion and electron power into the SOL (as in the 2-D simulations), $Q \sim 8.5$ is obtained, with required core fuelling increasing from 40 to 80 Pa m^3/s as the power is raised. Fig. 6 applies to fully-relaxed current profiles developed after 100's of seconds; before full relaxation, the Q values obtained are 15 and higher. At the higher n_s/n_{s_crit} and at the lower SOL powers, the Q is somewhat lower because of confinement degradation.

6. Geometry

The scaling results given here apply only to the geometry of Fig. 1. Preliminary scaling results for the geometry of [7], with a flat bottom of the divertor rather

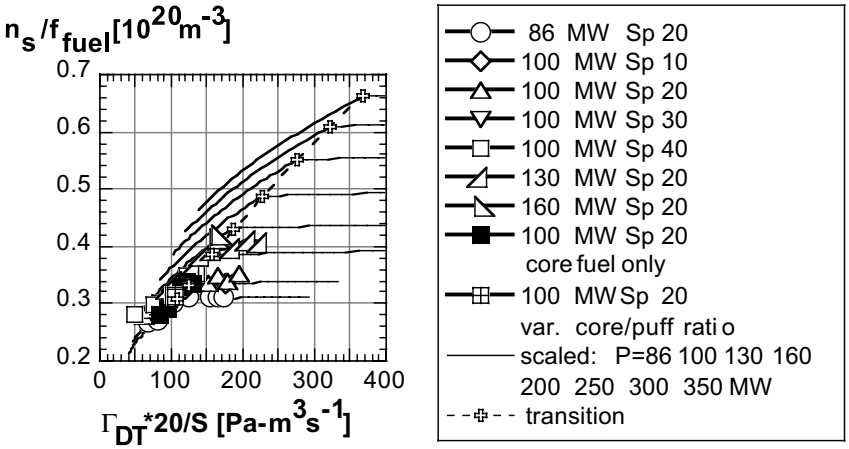

Fig. 7. Density versus throughput. Curves from the scalings and points of transition from regime A to regime B shown for SOL powers from 86 to 350 MW.

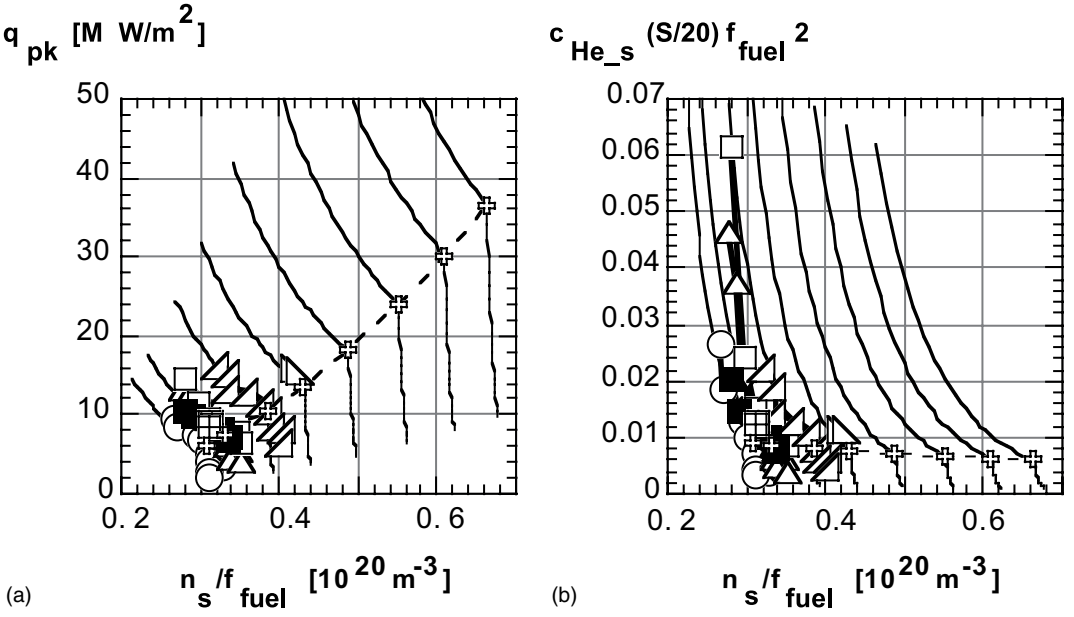

Fig. 8. (a) Peak power load and (b) helium concentration, versus density. Scaling and legend as in Fig. 7.

than a V-shape, yield the same scaling for peak power load (but 9% lower) and helium density, and a density scaling as Eq. (1) multiplied by a factor $S_{\#}^{0.11}/(1.03P_{\#}^{0.3})$ Future studies on the influence of geometry parameters on the scaling are required.

7. Extrapolation and conclusions

Nominal operation of ITER corresponds to $P_{\mathrm{SOL}} = 100$ MW, whereas reactor-like operation at 2 GW and $Q = 30$ would correspond to $P_{\mathrm{SOL}} = 330$ MW. The fit to the scalings and the extrapolations to reactor-like operation (if no additional physics, e.g. a ballooning limit on the SOL pressure gradient, needs to be included) are shown in Figs. 7 and 8. If full detachment can not be used because of confinement degradation of the core plasma, the highest usable density (pressure) will be the transition point. The operating point should be near the transition (i.e. edge density 0.65×10^{20} m^{-3}) because of the strong dependence of the peak power load (Fig. 8(a)), which would reach 35 MW/m^2 for reactor-like operation at the transition. Helium continues to be unproblematic (Fig. 8(b)); the margin to the allowable 6% concentration would allow simultaneous reduction of pumping speed (<10 m^3/s) and gas puff at constant divertor pressure and core fuelling to reduce tritium inventory. However, no trade-off of peak power against helium concentration is possible.

The key parameter for the scalings is the divertor neutral pressure. Preliminary indications show that the scalings depend also on the ratio of electron to ion power across the CEI (unity here), and that the saturation point for core-fuelled cases is higher than the scaling, i.e. depends on f_{fuel} (these cases do not yet saturate here). Both these effects, as well as the influence of the helium recycling on the core parameters, are being investigated further.

At constant pressure in the attached regime, both peak power load and helium density vary as the square of the power. At the transition point (higher pressure at higher power, i.e. constant detachment state), they vary as $P^{1.26}$ and $P^{0.26}$, respectively. A significant operating window exists at nominal operation of ITER. Inclusion of helium elastic collisions considerably alleviates the helium removal problem. The 2D simulation parameters near the transition density are reasonably consistent with core operation at $Q \sim 10$. An improved criterion defining the allowable detachment at high power is required. Future work will concentrate on core-edge consistency, solutions for higher power operation, and impurity seeding and realistic wall models for carbon to obtain lower peak power load.

References

[1] A.S. Kukushkin, H.D. Pacher, G. Janeschitz, et al., Proceedings of the 28th EPS Conference on Controlled Fusion and Plasma Physics, Madeira, 2001.
[2] A.S. Kukushkin, H.D. Pacher, Plasma Phys. Control. Fusion 44 (2002) 931.
[3] H.D. Pacher, W.D. D'haeseleer, G.W. Pacher, J. Nucl. Mater. 196–198 (1992) 457.

[4] S.I. Krasheninnikov et al., J. Nucl. Mater. 266–269 (1999) 251.
[5] G.W. Pacher, H.D. Pacher, G. Janeschitz, et al., Proceedings of the 28th EPS Conference on Controlled Fusion and Plasma Physics, Madeira, 2001.
[6] G. Janeschitz, G.W. Pacher, et al., Plasma Phys. Control. Fusion 44 (5A) (2002) A459.
[7] A.S. Kukushkin, G. Janeschitz, A. Loarte, H.D. Pacher, et al., J. Nucl. Mater. 290–293 (2001) 887.